

Synthesis, Characterization and Docking Study of Novel Pyrimidine Derivatives as Anticancer Agents

Manal Mohamed Talaat El-Saidi¹, Ahmed Ali El-Sayed^{1,2,*}, Erik Bjerregaard Pedersen², Mohamed Abdelhamid Tantawy^{3,4}, Nadia Ragab Mohamed¹, and Wafaa Ahmed Gad¹

¹Photochemistry Department, Chemical Research Division, National Research Center, Dokki, Giza, 12622, Egypt

²Department of Physics, Chemistry, and Pharmacy, University of Southern Denmark, Campusvej 55, 5230 Odense M, Denmark

³Hormones Department, Medical Research Division, National Research Center, Dokki, Giza, 12622, Egypt

⁴Stem Cells Lab, Center of Excellence for Advanced Sciences, National Research Centre, Dokki, Giza, 12622, Egypt

* **Corresponding author:**

email: ahmedcheme4@yahoo.com

Received: October 15, 2019

Accepted: November 18, 2019

DOI: 10.22146/ijc.50582

Abstract: New compounds **5** and **9** using DNA bases e.g. Adenine **1** and Guanine **6** derivatives have been synthesized. The use of simple methods to synthesize compounds **5** and **9** were done using pyrimidine as an alternative DNA base ring. Another design to synthesize new simple pyrimidine rings utilizing thiourea and ethylcyano acetate to afford 6-amino-2-thiouracil was adopted. The reaction of thiouracil **10** with chloro cyano or chloro ester and ketone, resulted in the formation of adduct compounds **18-21**, rather than the formation of compound **17**. All the synthesized compounds were subjected to docking study, in order to gain insights into their binding modes against cyclin-dependent protein kinase 2 (CDK-2) that is involved heavily in cell cycle regulation and receptor protein B-cell lymphoma 2 (BCL-2) which is involved in cell apoptosis. These targets were selected based on their key roles in cancer progression via the regulation of the cell cycle and DNA replication. Molecular-docking analyses showed that compound **14e** was the best docked ligand against both targets, as it displayed the lowest binding energy, critical hydrogen bonds and hydrophobic interactions with the targets.

Keywords: DNA; guanidine; adenine; 6-aminothiouracil; hydrazonoyl halides; thiadiazole; phenylisocyanate; molecular docking

■ INTRODUCTION

Modification of DNA and RNA oligonucleotides with new synthesized heterocyclic compounds have drawn significant interest owing to their ability to imitate new gene chemical probes that play an important role in the drug discovery process [1-7]. Gene-therapy in recent research was based on DNA and its modification [8-10]. The thymidine ring is a DNA building block that interests many researchers to focused their research on the synthesis of new pyrimidine rings as anti-cancer agents such as 5-fluorouracil [1-14], and anti-HIV like AZT, D4T, Nikavir [15-21], Lamivudina [22] and Emtricitabina [16,23-24]. The Nitrogen containing heterocycles like pyrimidines and their derivatives have received great

attention for their considerable exciting biological activities [25-28]. Several pyrimidines have been isolated from the nucleic acid hydrolysis. The nucleic acids are an essential constituent of cells. So, pyrimidines are found to be present in RNA and DNA [29]. In addition to this, the pyrimidine ring is also found in vitamin B₁ and other derivatives are used as hypnotics [30]. The literature survey indicated that compounds having pyrimidine nucleus possess a broad range of biological activities [31-35]. On the other hand, hydrazonoyl halides (pyrimidine nucleobase) are versatile synthons for many heterocycles that have found many applications in both the industrial and pharmaceutical fields [36-38]. As a precursor of bioactive heterocycles

[39-40], this report is concerned with the synthesis of new types of bioactive heterocycles using thiouracils.

This work is carried out in order to further modify our previously prepared pyrimidine ring bases heterocyclic compounds in order to increase their bioactivity. The main strategy is the chemical synthesis is described technically; while the biological activity is accomplished by molecular docking. This technique provides a rapid way to evaluate the likely binders from large chemical libraries with minimal costs and it is being widely used as a vital component of the drug discovery process [41]. Molecular docking study has been utilized to determine the possible mechanism action of the tested compounds against two proteins cyclin-dependent protein kinase 2 (CDK-2) and receptor protein B-cell lymphoma 2 (BCL-2) that are implicated significantly in cancer progression.

■ EXPERIMENTAL SECTION

Chemistry

All solvents were purified and dried before use. All melting points were uncorrected and measured using Electro-Thermal IA 9100 apparatus (Shimadzu, Japan). Infrared spectra were recorded as potassium bromide pellets on a Perkin-Elmer 1650 spectrophotometer, National Research Centre, Cairo, Egypt. ¹H-NMR spectra were recorded on a Jeol-Ex-500 NMR spectrometer and chemical shifts were expressed as part per million; (δ values, ppm) against TMS as an internal reference, National Research Centre, Cairo, Egypt. Mass spectra were recorded on EI + Q1 MSLMR UPLR, National Research Centre, Cairo, Egypt. Microanalyses were operated using the Mario Elmentar apparatus, Organic Microanalysis Unit, National Research Center, Cairo, Egypt.

Procedure

General procedure for compounds 3 and 7

To a solution of 8-bromo-2'-deoxyguanosine (**1**) or 8-bromo-2'-deoxyadenosine (**6**) (0.478 mmol) in dry DMF (30 mL), N-(4-pentynyl)-phthalimide (1.71 mmol) was added under argon gas and then copper iodide (0.25 mmol), Pd(PPh₃)₄ (0.0515 mmol) and triethylamine (1.43 mmol) were added to the reaction mixture. The

reaction was stirred at 55 °C under argon till the reaction was finished according to TLC analysis. The product was separated by evaporation of the solvent and the residue was purified by silica gel (size 230–400 mesh) column chromatography, and carried out starting from dichloromethane and increasing the polarity until the product was collected using TLC and the column was washed with MeOH.

2-{5-[2-Amino-9-(4-hydroxy-5-hydroxymethyl-tetrahydro-furan-2-yl)-6-oxo-6,9-dihydro-1H-purin-8-yl]-pent-4-ynyl}-isoindole-1,3-dione **3.** Yellow foam (silica column DCM/MeOH 7:3) yield 90%. IR spectrum (KBr, ν , cm⁻¹): 3432 (-OH); 3098 (C-H, aromatic); 1690 (-C=O); 1675 (-C=O). ¹H NMR (CDCl₃-d, δ ppm): 10.75 (s, 1H, -OH, sugar); 7.79–7.87 (m, 4H, aromatic protons); 6.48 (s, 1H, -NH); 6.23–6.27 (t, J = 6.25, 2H, -CH₂); 5.21–5.20 (d, J = 5.21, 2H, -CH₂); 4.84–4.87 (t, J = 4.85, 2H, -CH₂); 2.89 (s, 2H, NH₂); 2.56–2.62 (t, J = 5.26, 1H, sugar proton); 2.99–3.06 (m, 1H, sugar proton); 2.08–2.14 (m, 1H, sugar proton); 3.38–3.62 (m, 1H, sugar proton); 3.85–3.62 (m, 1H, sugar proton); 2.73 (s, 1H, -CH₂-OH, sugar); 1.13–1.18 (m, 2H, -CH₂); ¹³C-NMR (CDCl₃-d, δ ppm) 16.43 (-CH₂-CH₂-), 34.06 (-N-CH₂-CH₂-), 38.81 (-N-CH₂-CH₂-), 40.06 (-CH-CH₂-CH-), 61.58 (-CH-O-), 63.81(-CH₂-O-), 65.66 (-CH₂-OH), 81.48 (-C≡C-), 85.45 (-C≡C-), 87.51 (-N-CH-O-), 120.14, 122.40, 125.43, 122.88, 131.62, 134.13 (aromatic carbon), 148.08 (-N-C-C=O), 149.90 (-N-C-N-), 153.77 (-N=C-N), 167.90 (NH₂-C=N-), 168.31(-C=O), 180.10 (-C=O), 182.22 (NH-C=O). MS, m/z (%): 464. Anal. Calcd. for C₂₃H₂₂N₆O₆ (464.43): C, 57.74; H, 4.63; N, 17.56. Found: C, 57.60; H, 4.55; N, 17.43.

2-{5-[6-Amino-9-(4-hydroxy-5-hydroxymethyl-tetrahydro-furan-2-yl)-9H-purin-8-yl]-pent-4-ynyl}-isoindole-1,3-dione **7.** Brown foam (silica column DCM/MeOH, 6:4) yield 95%. IR spectrum (KBr, ν , cm⁻¹): 3445 (-NH₂); 3432 (-OH); 3098 (C-H, aromatic); 1700 (-C=O); 1680 (-C=O). ¹H-NMR (CDCl₃-d, δ ppm): 8.31 (s, 1H, -OH); 7.84–7.90 (m, 1H, aromatic protons); 7.70–7.73 (m, 1H, aromatic protons); 7.29 (s, 1H, pyrimidine proton); 6.78–6.87 (m, 2H, aromatic protons); 6.47 (s, 2H, -NH₂); 4.30 (s, 1H, -OH); 3.90–

3.93 (t, $J = 3.91$, 2H, $-\text{CH}_2$); 4.49 (d, $J = 3.21$, 2H, $-\text{CH}_2$); 3.82–3.85 (t, $J = 3.91$, 2H, $-\text{CH}_2$); 2.73 (s, 1H, $-\text{OH}$); 2.56–2.62 (t, $J = 5.26$, 1H, sugar proton); 2.99–3.06 (m, 1H, sugar proton); 2.08–2.14 (m, 1H, sugar proton); 3.38–3.62 (m, 1H, sugar proton); 3.85–3.62 (m, 1H, sugar proton); 2.06–2.11 (m, 2H, $-\text{CH}_2$). ^{13}C -NMR (CDCl_3 -d, δ ppm): 16.99 ($-\text{CH}_2$), 26.51 ($-\text{CH}_2$), 36.76 ($-\text{CH}_2$, sugar), 40.54 ($-\text{CH}_2$), 50.54 ($-\text{CH}_2$ -OH), 63.66 (CH-OH), 70.31 ($-\text{C}\equiv\text{C}$ -), 70.66 ($-\text{CH}$ -N, sugar), 87.51 ($-\text{CH}$, sugar), 90.14 ($-\text{C}\equiv\text{C}$ -), 97.21, 120.02, 123.50 (aromatic carbon), 131.75 ($-\text{C}-\text{NH}_2$), 134.78 ($-\text{N}-\text{C}-\text{N}$, imidazole), 148.22 ($-\text{N}-\text{C}-\text{N}$, Pyrimidine), 152.58 (C-N, pyrimidine), 155.67 (C-N, pyrimidine), 168.83 (2-C=O). MS, m/z (%): 462. Anal. Calcd. for $\text{C}_{23}\text{H}_{22}\text{N}_6\text{O}_5$ (462.46): C, 59.73; H, 4.79; N, 18.17. Found: C, 59.62; H, 4.59; N, 18.01.

General procedure for compounds 4 and 8

The compounds 3 and 7 were co-evaporated with anhydrous pyridine (3 × 4 mL) and dissolved in dry pyridine (2 mL). The resulting solution was protected from moisture, purged with argon and placed in an ice bath. TMS-Cl (0.55 mL) was added dropwise *via* syringe. The mixture was stirred for 2 h at room temperature. After that, the solution was cooled in an ice bath and isobutyric anhydride (0.13 mL) was added dropwise. The solution was stirred for 2 h in room temperature, and the product was purified from the mixture by silica gel (size 230–400 mesh) column chromatography. Columns were carried out starting from dichloromethane and increasing the polarity until the product was collected using TLC and the column was washed with MeOH.

N-[8-[5-(1,3-Dioxo-1,3-dihydro-isoindol-2-yl)-pent-1-ynyl]-9-(4-hydroxy-5-hydroxymethyl-tetrahydro-furan-2-yl)-6-oxo-6,9-dihydro-1H-purin-2-yl]-isobutyramide 4.

White ppt. (column DCM/MeOH, 8:2) yield 95%. IR spectrum (KBr, ν , cm^{-1}): 3432 ($-\text{OH}$); 3145 ($-\text{NH}$); 3098 (C-H, aromatic); 2895 (C-H, aliphatic), 1700 ($-\text{C}=\text{O}$); 1690 ($-\text{C}=\text{O}$); 1680 ($-\text{C}=\text{O}$). ^1H -NMR (CDCl_3 -d, δ ppm): 12.16 (s, 1H, $-\text{OH}$, sugar); 7.79–7.86 (m, 4H, aromatic protons); 6.63 (s, 1H, $-\text{NH}$); 6.35–6.31 (t, $J = 6.34$, 2H, $-\text{CH}_2$); 5.25, 5.24 (d, $J = 5.25$, 2H, $-\text{CH}_2$); 4.74 (s, 1H, NH); 4.84–4.87 (t, $J = 4.85$, 2H, $-\text{CH}_2$); 4.43 (s, 1H $\text{CH}(\text{CH}_3)_2$); 3.85–3.62 (m, 1H, sugar proton); 3.38–3.62 (m, 1H, sugar proton); 2.99–3.06 (m, 1H, sugar proton); 2.73 (s, 1H,

CH_2 -OH); 2.56–2.62 (t, $J = 5.26$, 1H, sugar proton); 2.08–2.14 (m, 1H, sugar proton); 1.13–1.18 (m, 2H, $-\text{CH}_2$); 1.05 (s, 3H, CH_3); 1.07 (s, 3H, CH_3). ^{13}C -NMR (CDCl_3 -d, δ ppm): 7.89 ($-\text{CH}_3$), 10.24 ($-\text{CH}_3$), 18.50 ($-\text{CH}_2$ - CH_2 -), 35.16 ($-\text{N}-\text{CH}_2$ - CH_2 -), 39.91 ($-\text{N}-\text{CH}_2$ - CH_2 -), 42.06 ($-\text{CH}-\text{CH}_2$ - CH -), 52.02 ($-\text{CH}-\text{CH}_3$), 62.08 ($-\text{CH}-\text{O}$ -), 66.91 ($-\text{CH}_2$ -O-), 65.09 ($-\text{CH}_2$ -OH), 80.41 ($-\text{C}\equiv\text{C}$ -), 85.95 ($-\text{C}\equiv\text{C}$ -), 88.21 ($-\text{N}-\text{CH}-\text{O}$ -), 120.14, 122.40, 122.88, 125.43, 131.62, 134.13 (aromatic carbon), 147.08 ($-\text{N}-\text{C}-\text{C}=\text{O}$), 149.02 ($-\text{N}-\text{C}-\text{N}$ -), 153.90 ($-\text{N}=\text{C}-\text{N}$), 167.11 (NH_2 - $\text{C}=\text{N}$ -), 168.31 ($-\text{C}=\text{O}$), 180.10 ($-\text{C}=\text{O}$), 182.02 ($\text{NH}-\text{C}=\text{O}$), 183.90 ($\text{NH}-\text{C}=\text{O}$). MS, m/z (%): 549. Anal. Calcd. for $\text{C}_{27}\text{H}_{28}\text{N}_6\text{O}_7$ (548.55): C, 59.12; H, 5.14; N, 15.32. Found: C, 59.01; H, 5.03; N, 15.12.

N-[8-[5-(1,3-Dioxo-1,3-dihydro-isoindol-2-yl)-pent-1-ynyl]-9-(4-hydroxy-5-hydroxymethyl-tetrahydro-furan-2-yl)-9H-purin-6-yl]-isobutyramide 8.

Yellow foam (column DCM/MeOH 6:4) yield 86%. IR spectrum (KBr, ν , cm^{-1}): 3401 ($-\text{OH}$); 3090 (C-H, aromatic); 1690 ($-\text{C}=\text{O}$); 1679 ($-\text{C}=\text{O}$). ^1H NMR (CDCl_3 -d, δ ppm): 8.88 (s, 1H, $-\text{OH}$); 8.70 (s, 1H, pyrimidine proton); 7.72–7.74 (m, 2H, aromatic protons); 7.85–7.87 (m, 2H, aromatic protons); 7.26 (s, 1H, $-\text{NH}$); 6.91–6.95 (m, 1H, sugar); 4.79, 4.80 (d, $J = 4.80$, 1H, sugar); 4.33 (s, 2H, CH_2 -OH); 3.83–3.99 (t, $J = 4.96$, 2H, $-\text{CH}_2$); 3.82–3.85 (t, $J = 3.91$, 2H, $-\text{CH}_2$); 3.38–3.62 (m, 1H, sugar proton); 3.85–3.62 (m, 1H, sugar proton); 2.73 (s, 1H, $-\text{OH}$); 2.56–2.62 (t, $J = 5.26$, 1H, sugar proton); 2.06–2.11 (m, 2H, $-\text{CH}_2$); 1.29 (s, 1H, $\text{CH}(\text{CH}_3)_2$); 1.21 (s, 3H, CH_3); 1.18 (s, 3H, CH_3). ^{13}C -NMR (CDCl_3 -d, δ ppm): 17.04 ($-\text{CH}_2$ - $\text{C}\equiv\text{C}$ -), 26.40 (2- CH_3), 33.76 ($-\text{CH}_2$, sugar), 36.70 ($-\text{CH}_2$ -N), 43.63 ($-\text{CH}_2$ -OH), 63.62 (CH -OH), 70.11 ($-\text{C}\equiv\text{C}$ -), 87.71 ($-\text{CH}-\text{N}$, sugar), 90.29 ($-\text{CH}$, sugar), 98.91 ($-\text{C}\equiv\text{C}$ -), 122.36, 123.57, 131.74, 134.42, 136.57, 147.89, 149.34, 152.57 (aromatic carbon), 168.89 ($-\text{C}=\text{O}$), 175.92 ($-\text{C}=\text{O}$), 180.00 ($-\text{C}=\text{O}$). MS, m/z (%): 532. Anal. Calcd. for $\text{C}_{27}\text{H}_{28}\text{N}_6\text{O}_6$ (532.21): C, 60.89; H, 5.30; N, 15.78. Found: C, 60.71; H, 5.21; N, 15.65.

General procedure for compounds 5 and 9

The compounds 4 and 8 were co-evaporated with anhydrous pyridine (3 × 3 mL) and dissolved in dry pyridine (10 mL). The DMT-Cl (3.6 mmol) was dissolved in dry pyridine (3 mL) and added to the

nucleoside solution dropwise in an ice bath over 2.5 h and the reaction mixture was stirred in an ice bath until the TLC was finished. The product was separated and purified with flash column silica gel (size 230–400 mesh) column chromatography. The column was carried out starting from dichloromethane with a few drops of triethylamine (Et₃N) and increasing the polarity until the product was collected using TLC and the column was washed with methanol.

N-{9-[5-[Bis-(4-methoxy-phenyl)-phenyl-methoxymethyl]-4-hydroxy-tetrahydro-furan-2-yl]-8-[5-(1,3-dioxo-1,3-dihydro-isoindol-2-yl)-pent-1-ynyl]-6-oxo-6,9-dihydro-1H-purin-2-yl]-isobutyramide 5. White ppt. (column DCM/MeOH 7:3) yield 55%. IR spectrum (KBr, ν , cm⁻¹): 3432 (–OH); 3140 (–NH); 3098 (C–H, aromatic); 2895 (C–H, aliphatic), 1710 (–C=O); 1697 (–C=O); 1681 (–C=O). ¹H-NMR (CDCl₃-d, δ ppm): 8.34 (s, 1H, NH); 7.79–7.86 (m, 5H, aromatic protons); 7.13–7.17 (m, 4H, aromatic protons); 7.27, 7.31 (d, J = 6.68, 2H, aromatic protons); 7.35, 7.38 (d, J = 6.68, 2H, aromatic protons); 6.67, 6.69 (d, J = 6.68, 2H, aromatic protons); 6.73, 6.76 (d, J = 6.68, 1H, aromatic protons); 6.63 (s, 1H, –NH); 6.35–6.31 (t, J = 6.35, 2H, –CH₂); 6.40–6.43 (t, J = 6.42, 1H, –CH, sugar); 5.39, 5.36 (d, J = 5.28, 1H, sugar); 5.34 (s, 1H, –OH, sugar); 4.84–4.87 (t, J = 4.85, 2H, –CH₂); 4.43 (s, 1H, CH(CH₃)₂); 3.85–3.62 (m, 1H, sugar proton); 3.68 (s, 3H, –OCH₃); 3.70 (s, 3H, –OCH₃); 2.73 (s, 2H, CH₂-ODMT); 2.56–2.62 (t, J = 5.26, 1H, sugar proton); 2.08–2.14 (m, 1H, sugar proton); 1.13–1.18 (m, 2H, –CH₂); 1.05 (s, 3H, CH₃); 1.07 (s, 3H, CH₃). ¹³C-NMR (CDCl₃-d, δ ppm) 7.89 (–CH₃), 10.24 (–CH₃), 18.50 (–CH₂–CH₂–), 35.16 (–N–CH₂–CH₂–), 39.91 (–N–CH₂–CH₂–), 42.06 (–CH–CH₂–CH–), 52.02 (–CH–CH₃), 58.72 (2–OCH₃); 62.08 (–CH–O–), 66.91 (–CH₂–O–), 65.09 (–CH₂–OH), 80.41 (–C≡C–), 85.95 (–C≡C–), 88.21 (–N–CH–O–), 90.79 (Ph–C–O), 120.14, 123.25, 123.01, 122.40, 122.88, 125.43, 131.62, 134.13, 136.35, 137.60, 138.37, 139.37, 141.09, 140.17, 142.84 (aromatic carbons), 147.08 (–N–C–C=O), 149.02 (–N–C–N–), 153.90 (–N=C–N), 167.11 (NH₂–C=N–), 168.31 (–C=O), 180.10 (–C=O), 182.02 (NH–C=O), 183.90 (NH–C=O). MS, m/z (%): 850. Anal. Calcd. for C₄₈H₄₆N₆O₉ (850.91): C, 67.75; H, 5.45; N, 9.88. Found: C, 67.51; H, 5.22; N, 9.65.

N-{9-[5-[Bis-(4-methoxy-phenyl)-phenyl-methoxymethyl]-4-hydroxy-tetrahydro-furan-2-yl]-8-[5-(1,3-dioxo-1,3-dihydro-isoindol-2-yl)-pent-1-ynyl]-9H-purin-2-yl]-isobutyramide 9. White foam (column DCM/MeOH 4:6) yield 60%. IR spectrum (KBr, ν , cm⁻¹): 3401 (–OH); 3090 (C–H, aromatic); 1675 (–C=O); 1673 (–C=O). ¹H-NMR (CDCl₃-d, δ ppm): 8.44 (s, 1H, –NH); 7.84 (s, 1H, pyrimidine proton); 7.83–7.78 (m, 2H, aromatic protons); 7.70–7.72 (m, 2H, aromatic protons); 7.39–7.41 (m, 2H, aromatic protons); 7.27–7.30 (m, 2H, aromatic protons); 7.17–7.23 (m, 4H, aromatic protons); 6.73–6.80 (m, 5H, aromatic protons); 4.79, 4.80 (d, J = 4.80, 1H, sugar); 4.33 (s, 2H, CH₂); 4.23–4.30 (m, 1H, sugar); 3.83–3.99 (t, J = 4.96, 2H, –CH₂); 3.82–3.85 (t, J = 3.91, 2H, –CH₂); 3.77 (s, 3H, –OCH₃); 3.76 (s, 3H, –OCH₃); 3.38–3.62 (m, 1H, sugar proton); 3.85–3.62 (m, 1H, sugar proton); 2.73 (s, 1H, –OH); 2.56–2.62 (t, J = 5.26, 1H, sugar proton); 2.06–2.11 (m, 2H, –CH₂); 1.29 (s, 1H, CH(CH₃)₂); 1.21 (s, 3H, CH₃); 1.18 (s, 3H, CH₃). ¹³C-NMR (CDCl₃-d, δ ppm): 17.04 (–CH₂–C≡C–), 19.19 (–CH₃), 26.40 (–CH₃), 33.76 (–CH₂, sugar), 36.70 (–CH₂–N), 43.63 (–CH₂–ODMT), 55.72 (2–OCH₃); 63.62 (CH–OH), 70.11 (–C≡C–), 87.71 (–CH–N, sugar), 98.11 (–CH, sugar), 100.00 (–C≡C–), 122.36, 123.57, 126.76, 127.72, 128.22, 129.99, 130.08, 131.84, 134.27, 136.00, 136.07, 144.77, 147.89, 148.84, 150.37, 152.37 (aromatic carbon), 168.89 (–C=O), 175.92 (–C=O), 180.00 (–C=O). MS, m/z (%): 834. Anal. Calcd. for C₄₈H₄₆N₆O₈ (834.91): C, 69.05; H, 5.55; N, 10.07. Found: C, 68.98; H, 5.40; N, 9.90.

General procedure for 14a-f

Sodium hydride (2 mmol) and carbon disulphide (1 mmol) was added to uracil (1 mmol) in 15 mL DMF; the reaction mixture was stirred overnight to have compound **11** (not isolated from the reaction mixture). The hydrazonyl halides (1 mmol) was added to the non-isolated compound **11**. The reaction mixture was stirred overnight then added with 15 mL of 1 M HCl to obtain crude solid of **14a-f**.

5-(6-Oxo-2-thioxo-1,2,3,6-tetrahydro-pyrimidin-4-ylimino)-4-tolyl-4,5-dihydro[1,3,4]thiadiazole-2-carboxylic acid phenylamide 14a. Yellow crystal (crystallization from benzene/petroleum ether), yield

72%; m.p. 250–252 °C. IR spectrum (KBr, ν , cm^{-1}): 3332 (–NH); 3098 (C–H, aromatic); 1672 (C=O), 1664 (C=O). $^1\text{H-NMR}$ (DMSO- d_6 , δ ppm): 2.63 (s, 3H, –CH₃); 5.34 (s, 1H, pyrimidine proton); 7.15–7.62 (m, 5H, aromatic-H); 7.82 (d, 2H, Ar-H); 7.96 (d, 1H, Ar-H); 11.74 (s, 1H, NH); 12.08 (s, 1H, NH); 14.02 (s, 1H, NH). $^{13}\text{C-NMR}$ (DMSO- d_6 , δ ppm): 26.56 (–CH₃); 103.56 (O=C–C–C, pyrimidine ring); 129.75, 130.25, 131.71, 137.21, 139.40, 141.50, 144.22, 149.2 (aromatic carbons); 161.22 (S–C–N); 173.98 (N=C–S); 178.83 (HN–C–N); 180.21 (C=O), 185.11 (C=S), 198.23 (C=O). MS, m/z (%): 436, 331, 316. Anal. Calcd. for C₂₀H₁₆N₆O₂S₂ (436.51): C, 55.03; H, 3.69; N, 19.25, S, 14.69. Found: C, 54.98; H, 3.59; N, 19.01, S 14.58.

6-(5-Acetyl-3-phenyl-3H-[1,3,4]thiadiazol-2-ylidene amino)-2-thioxo-2,3-dihydro-1H-pyrimidin-4-one 14b.

Yellow crystal (crystallization from ethanol), yield 77%; m.p. 220–222 °C. IR spectrum (KBr, ν , cm^{-1}): 3298 (–NH); 3118 (C–H, aromatic); 2980 (C–H, aliphatic); 1680 (C=O); 1670 (C=O). $^1\text{H-NMR}$ (DMSO- d_6 , δ ppm): 2.58 (s, 3H, –CH₃); 5.60 (s, 1H, pyrimidine proton); 7.11–7.66 (m, 5H, aromatic-H); 11.84 (s, 1H, NH); 12.04 (s, 1H, NH). $^{13}\text{C-NMR}$ (DMSO- d_6 , δ ppm): 25.91 (–CH₃); 106.56 (O=C–C–C, pyrimidine ring); 120.75, 122.25, 149.2 (aromatic carbons); 160.22 (S–C–N); 170.98 (N=C–S); 178.83 (HN–C–N); 182.21 (C=O), 188.11 (C=S), 198.23 (C=O). MS, m/z (%): 345 (77%); 268 (100%). Anal. Calcd. for C₁₄H₁₁N₅O₂S₂ (345.40): C, 48.68; H, 3.21; N, 20.28; S, 18.57. Found: C, 48.42; H, 3.02; N, 20.07, S, 18.38.

6-(5-Benzoyl-3-p-tolyl-3H-[1,3,4]thiadiazol-2-ylidene amino)-2-thioxo-2,3-dihydro-1H-pyrimidin-4-one 14c.

Brown crystal (crystallization from toluene), yield 68%; m.p. 210–212 °C. IR spectrum (KBr, ν , cm^{-1}): 3350 (–NH); 3009 (C–H, aromatic); 2920 (C–H, aliphatic); 1700 (C=O); 1668 (C=O). $^1\text{H-NMR}$ (DMSO- d_6 , δ ppm): 1.59 (s, 3H, –CH₃); 5.57 (s, 1H, pyrimidine proton); 7.14–7.66 (m, 5H, aromatic-H); 7.92–7.95 (d, 2H, aromatic CH); 8.29–8.32 (d, 2H, aromatic CH); 11.44 (s, 1H, NH); 12.15 (s, 1H, NH). $^{13}\text{C-NMR}$ (DMSO- d_6 , δ ppm): 29.50 (–CH₃); 101.75 (O=C–C–C, pyrimidine ring); 132.72, 135.21, 138.81, 139.21, 140.49, 146.56, 147.88, 151.21 (aromatic carbons); 165.26 (S–C–N); 170.78 (N=C–S); 177.89 (HN–C–N); 181.98 (C=O), 187.36 (C=S), 205.40 (C=O). MS, m/z (%): 424 (23%); 423 (3.6%); 422 (26%); 421 (50%). Anal.

Calcd. for C₂₀H₁₅N₅O₂S₂ (421.49): C, 56.99; H, 3.59; N, 16.62; S, 15.22. Found: C, 56.74; H, 3.44; N, 16.51; S, 15.01.

6-[3-Phenyl-5-(thiophene-2-carbonyl)-3H-[1,3,4]thiadiazol-2-ylideneamino]-2-thioxo-2,3-dihydro-1H-pyrimidin-4-one 14d.

Ball yellow crystal (benzene), yield 72%; m.p. 155–157 °C. IR spectrum (KBr, ν , cm^{-1}): 3384 (–NH); 3097 (C–H, aromatic); 2921 (C–H, aliphatic); 1680 (C=O); 1672 (C=O). $^1\text{H-NMR}$ (DMSO- d_6 , δ ppm): 5.64 (s, 1H, pyrimidine proton); 6.90–7.26 (m, 3H, thiophene-H); 7.42–7.80 (m, 5H, aromatic-H); 11.35 (s, 1H, NH); 12.13 (s, 1H, NH). $^{13}\text{C-NMR}$ (DMSO- d_6 , δ ppm): 105.96 (O=C–C–C, pyrimidine ring); 120.65, 125.32, 129.71, 137.40 (aromatic carbons); 138.60, 139.89, 147.51, 149.56 (Thiophene ring); 167.20 (HN–C–N); 175.98 (N=C–S); 183.21 (C=O), 187.11 (C=S), 198.23 (C=O). MS, m/z (%): 413 (23%); 412 (3.6%). Anal. Calcd. for C₁₇H₁₁N₅O₂S₃ (413.50): C, 49.38; H, 2.68; N, 16.94; S 23.26. Found: C, 49.18; H, 2.45; N, 16.75; S, 23.07.

6-[5-(Naphthalene-2-carbonyl)-3-phenyl-3H-[1,3,4]thiadiazol-2-ylideneamino]-2-thioxo-2,3-dihydro-1H-pyrimidin-4-one 14e.

Ball yellow (crystallization from benzene) yield 67%; m.p. 230–232 °C. IR spectrum (KBr, ν , cm^{-1}): 3390 (–NH); 3085 (C–H, aromatic); 2940 (C–H, aliphatic); 1690 (C=O); 1667 (C=O). $^1\text{H-NMR}$ (DMSO- d_6 , δ ppm): 5.72 (s, 1H, pyrimidine-H); 7.36–7.68 (m, 5H, aromatic -H); 7.79–8.98 (m, 7H, naphthalene-H); 11.04 (s, 1H, NH); 12.20 (s, 1H, NH). $^{13}\text{C-NMR}$ (DMSO- d_6 , δ ppm): 102.85 (O=C–C–C, pyrimidine ring); 127.32, 128.29, 129.70, 130.11, 131.71, 133.28, 134.91, 137.79, 139.59, 142.76, 146.81, 150.63 (aromatic carbons); 163.15 (S–C–N); 173.08 (N=C–S); 175.19 (HN–C–N); 182.18 (C=O), 189.86 (C=S), 203.58 (C=O). MS, m/z (%): 457 (23%). Anal. Calcd. for C₂₃H₁₅N₅O₂S₂ (457.53): C, 60.38; H, 3.30; N, 16.31. Found: C, 60.14; H, 3.18; N, 16.21.

6-(5-Benzoyl-3-phenyl-3H-[1,3,4]thiadiazol-2-ylidene amino)-2-thioxo-2,3-dihydro-1H-pyrimidin-4-one 14f.

Brown ppt. (crystallization from methanol) yield 66%; m.p. 209–212 °C. IR spectrum (KBr, ν , cm^{-1}): 3310 (–NH); 3090 (C–H, aromatic); 2950 (C–H, aliphatic); 1685 (C=O); 1661 (C=O). $^1\text{H-NMR}$ (DMSO- d_6 , δ ppm): 5.67 (s, 1H, pyrimidine proton); 7.04–8.12 (m, 10H, aromatic-H); 11.34 (s, 1H, NH); 12.01 (s, 1H, NH). $^{13}\text{C-NMR}$ (DMSO- d_6 , δ ppm): 105.65 (O=C–C–C, pyrimidine

ring); 129.70, 131.71, 134.91, 137.79, 139.59, 142.76, 146.81, 150.63 (aromatic carbons); 165.26 (S–C–N); 170.78 (N=C–S); 177.89 (HN–C–N); 181.98 (C=O), 187.36 (C=S), 205.40 (C=O). MS, *m/z* (%): 410 (10.2%); 408 (24.6%); 407 (23%). Anal. Calcd. for C₁₉H₁₃N₅O₂S₂ (407.47): C, 56.01; H, 3.22; N, 17.19. Found: C, 55.94; H, 3.02; N, 17.03.

General procedure for 18-21

Phenylisocyanate (1 mmol) was added to a solution of uracil (1 mmol) and potassium hydroxide (1 mmol) in 15 mL DMF; stirred overnight to afford non-isolated **16**. The non-isolated compound **16** was reacted with halo-compounds. After being stirred for 24 h, adducts **18-21** were precipitated as crude after treatment of the solution with 15 mL of iced 2 M HCl.

1-[6-Oxo-2-thioxo-1,2,3,6-tetrahydro-pyrimidin-4-yl]-3-phenyl-isothiourea 18. Dark brown (crystallization from benzene), Yield 55%; m.p. 210–211 °C. IR spectrum (KBr, ν , cm⁻¹): 3335 (–NH); 3031 (C–H, aromatic); 2976 (C–H, aliphatic); 1675 (C=O). ¹H-NMR (DMSO-d₆, δ ppm): 2.01 (s, 1H, SH); 5.42 (s, 1H, pyrimidine-H); 7.15–7.29 (m, 5H, aromatic-H); 7.89 (s, 1H, –NH); 10.79 (s, 1H, NH); 12.01 (s, 1H, NH). ¹³C-NMR (DMSO-d₆, δ ppm): 105.32 (O=C–C=C); 119.21, 125.21, 135.25, 142.21 (aromatic carbons); 171.64 (N=C–SH); 175.23 (C=O); 196.63 (C=S). MS, *m/z* (%): 280 (6.5%); 279 (22.4%); 278 (100%). Anal. Calcd. for C₁₁H₁₀N₄O₂S₂ (278.35): C, 47.46; H, 3.62; N, 20.13. Found: C, 47.25; H, 3.21; N, 20.07.

1-[6-Oxo-5-(2-oxo-2-phenyl-ethyl)-2-thioxo-1,2,3,6-tetrahydro-pyrimidin-4-yl]-3-phenyl-isothiourea 19. White crystals (crystallization from benzene/*n*-hexane), yield 75%; m.p. 239–241 °C. IR spectrum (KBr, ν , cm⁻¹): 3330 (–NH); 3029 (C–H, aromatic); 2986 (C–H, aliphatic); 1669 (C=O). ¹H-NMR (DMSO-d₆, δ ppm): 1.90 (s, 1H, –SH); 3.02 (s, 1H, –NH, pyrimidine, D₂O exchangeable); 3.55 (s, 2H, CH₂); 4.59 (s, 1H, –NH, D₂O exchangeable); 6.98–7.80 (m, 5H, aromatic-H); 7.82–8.52 (m, 5H, aromatic-H); 10.19 (s, 1H, –NH, pyrimidine). ¹³C-NMR (DMSO-d₆, δ ppm): 35.21 (–CH₂); 109.72 (O=C–C=C); 119.21, 125.21, 130.21, 142.75, 147.29, 149.33, 151.28, 159.98 (aromatic carbons); 168.22 (HN–C=C); 175.69 (HN–C–SH); 177.93 (C=O); 194.69 (C=S). MS, *m/z* (%): 398 (2.4%); 397 (22.4%); 396 (60.5%). Anal. Calcd. for C₁₉H₁₆N₄O₂S₂

(396.49): C, 57.56; H, 4.07; N, 14.13. Found: C, 57.35; H, 3.91; N, 14.09.

[4-Oxo-6-(3-phenyl-isothioureido)-2-thioxo-1,2,3,4-tetrahydro-pyrimidin-5-yl]-acetic acid ethyl ester 20. Dark red (crystallization from benzene), yield %; m.p. 203–205 °C. IR spectrum (KBr, ν , cm⁻¹): 3320 (–NH); 3055 (C–H, aromatic); 2985 (C–H, aliphatic); 1710 (C=O); 1670 (C=O). ¹H-NMR (DMSO-d₆, δ ppm): 1.18–1.25 (t, 3H, –CH₃); 2.08 (s, 1H, SH); 3.01 (s, 2H, CH₂); 4.10–4.20 (q, 2H, CH₂); 7.20–7.52 (m, 5H, aromatic-H); 8.28 (s, 1H, –NH); 11.34 (s, 1H, NH); 12.01 (s, 1H, NH). ¹³C-NMR (DMSO-d₆, δ ppm): 20.62 (–CH₃); 29.35 (–CH₂); 66.35 (–CH₂); 108.75 (O=C–C=C); 122.23, 128.21, 135.90, 150.89 (aromatic carbons); 163.72 (HN–C=C); 179.32 (C=O); 195.59 (S=C). MS, *m/z* (%): 366 (10.2%); 365 (24.6%); 364 (23%). Anal. Calcd. for C₁₅H₁₆N₄O₃S₂ (364.44): C, 49.43; H, 4.43; N, 15.37. Found: C, 49.12; H, 4.15; N, 15.10.

1-[6-Oxo-5-(2-oxo-2-propyl)-2-thioxo-1,2,3,6-tetrahydro-pyrimidin-4-yl]-3-phenyl-isothiourea 21. Dark brown ppt. (crystallization from benzene-*n*-hexane), yield 52%; m.p. 275–277 °C. IR spectrum (KBr, ν , cm⁻¹): 3285 (–NH); 3025 (C–H, aromatic); 2980 (C–H, aliphatic); 1702 (C=O); 1663 (C=O). ¹H-NMR (DMSO-d₆, δ ppm): 2.01 (s, 1H, SH); 2.61 (s, 3H, –CH₃); 2.98 (s, 2H, CH₂); 7.31–7.48 (m, 5H, aromatic-H); 7.95 (s, 1H, –NH); 9.86 (s, 1H, NH); 11.74 (s, 1H, NH). ¹³C-NMR (DMSO-d₆, δ ppm): 30.67 (–CH₃); 39.96 (–CH₂); 110.95 (O=C–C=C); 123.29, 130.98, 146.92, 152.99 (aromatic carbons); 178.77 (HN–C–N); 180.39 (C=O); 187.63 (HS–C–NH); 197.29 (S=C). MS, *m/z* (%): 336 (10.2%); 335 (24.6%); 334 (23%). Anal. Calcd. for C₁₄H₁₄N₄O₂S₂ (334.42): C, 50.28; H, 4.22; N, 16.75. Found: C, 50.02; H, 4.10; N, 16.35.

Molecular docking study

The structures of all tested compounds were modeled using the Chemsketch software (<http://www.acdlabs.com/resources/freeware/>) (Fig 1). The structures were optimized and energy minimized using the VEGAZZ software [43]. The optimized compounds were used to perform molecular docking. The three-dimensional structures of the two molecular targets (receptors) were obtained from the Protein Data Bank (PDB) (www.rcsb.org): CDK-2 (PDB: 1DI8,

<https://www.rcsb.org/pdb/explore/explore.do?structureId=1di8>), and BCL-2 (PDB:2O2F, <https://www.rcsb.org/pdb/explore/explore.do?structureId=2o2f>). The steps for receptor preparation included the removal of heteroatoms (solvent and ions), the addition of polar hydrogen and the assignment of Kollman charges. The active sites were defined using grid boxes of appropriate sizes around the bound cocystal ligands as is shown in Table 4. These compounds were docked into the active site of the CDK-2, and BCL-2 to study their interaction in silica and to correlate their anti-cancer activity. The docking study was performed using Auto dock vina, [44] and Chimera for visualization [45].

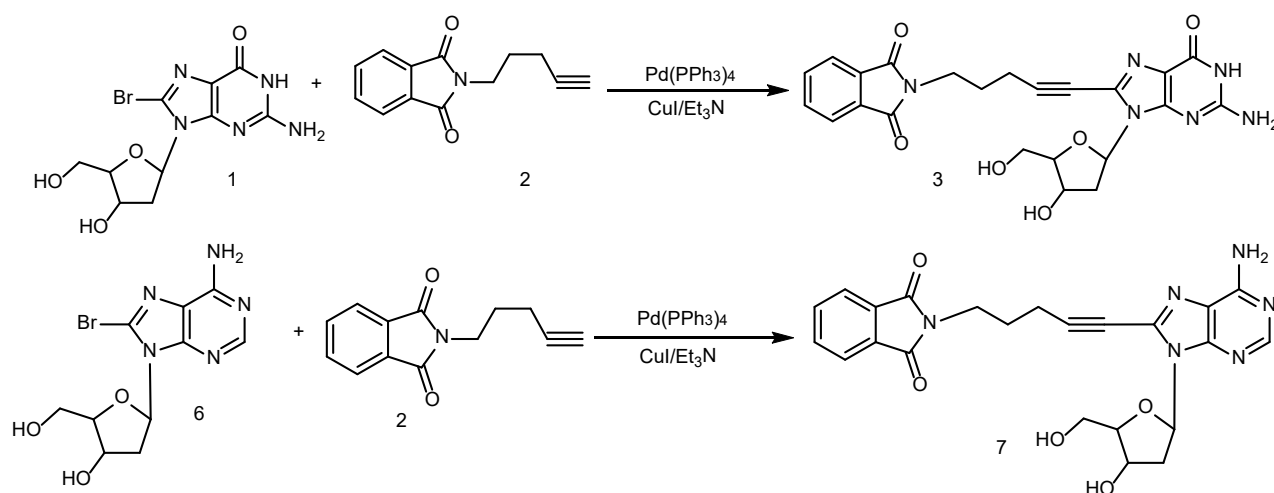
■ RESULTS AND DISCUSSION

From the modern therapeutic organic synthesis point of view and our previous work to modify DNA, [4-6] synthesis of modified DNA bases guanosine **1** and adenosine **6** derivatives was carried out. The Sonogashira reaction was carried out on the 2-pent-4-ynyl-isoindole-1,3-dione **2** with bromoguanosine **1** and bromoadenosine **6** using copper iodide and tetrakis(triphenylphosphine) palladium(0) Pd(PPh₃)₄ in the presence of triethyl amine to synthesize compound **3** and **7** (Scheme 1). The IR spectrum of compound **3** shows the amide carbonyl group at 1675 cm⁻¹, and the ¹H-NMR spectrum shows two triplets and one multiplet for the aliphatic -CH₂ groups at δ, ppm. 4.84–4.87 (t, *J* = 4.85, 2H, -CH₂); 1.13–1.18 (m, 2H, -CH₂); 6.23–6.27 (t, *J* = 6.25, 2H, -CH₂) and the

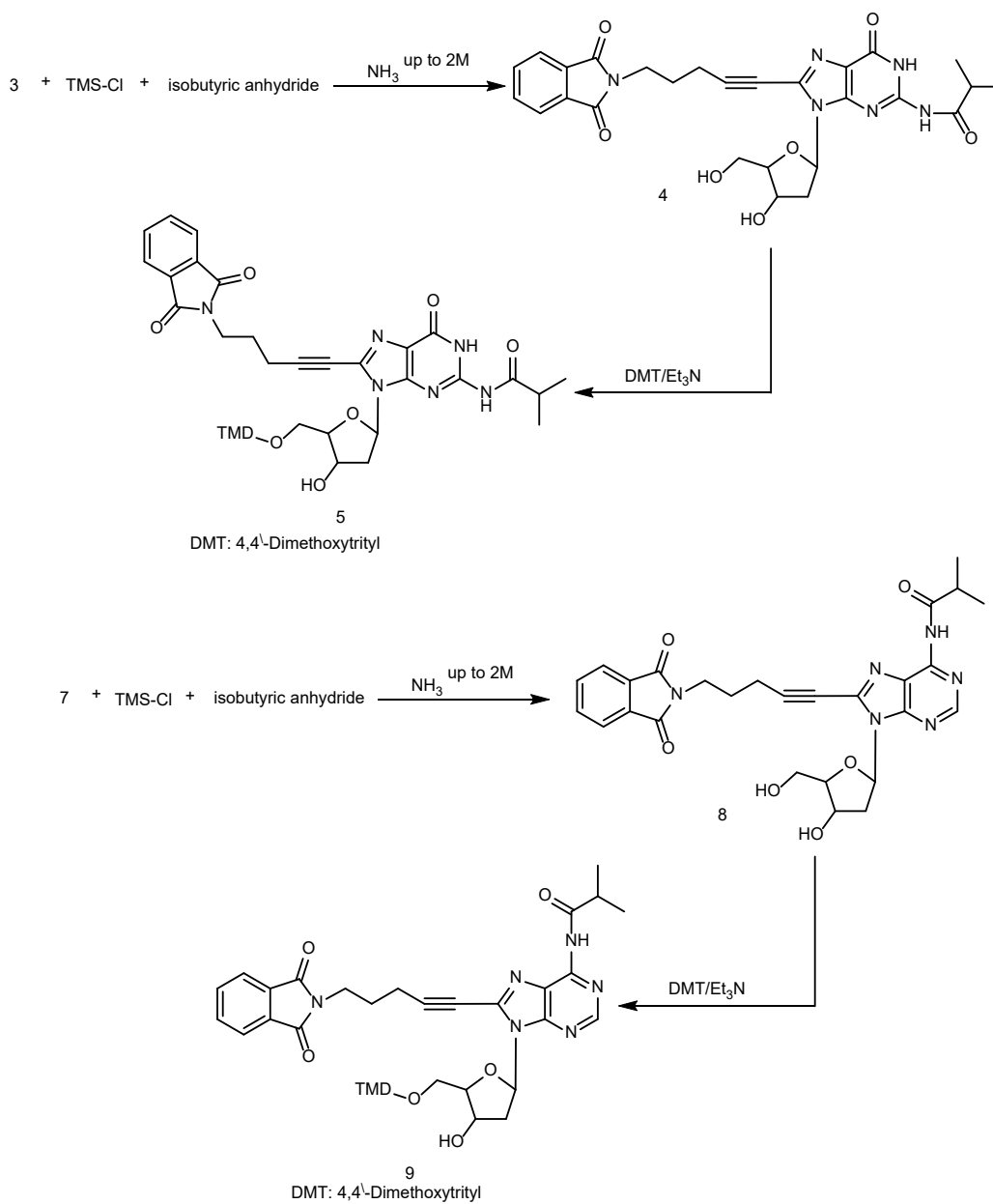
elemental analysis confirms the disappearance of bromine. The IR spectrum of compound **7** shows the amino group and the hydroxyl groups at 3445; 3432 cm⁻¹; and amide carbonyl group at 1680, and the ¹H-NMR shows singlet for the new -NH₂ at δ, ppm. 6.47 (s, 2H, -NH₂) and two triplets and one multiplet for the aliphatic -CH₂ groups at δ, ppm. 2.56–2.62 (t, *J* = 5.26, 1H, sugar proton); 2.99–3.06 (m, 1H, sugar proton); and the elemental analysis confirms the disappearance of bromine.

After that, the protection of -NH₂ groups of adenine and guanine with isobutyric anhydride in the presence of trimethylsilyl chloride (TMS-Cl) was carried out to have compounds **4** and **8**. On the other hand, the protection of the free hydroxyl sugar group (-CH₂OH) was carried out using 4,4'-dimethoxytrityl chloride (DMT-Cl) in the presence of triethyl amine to obtain the final corresponding modified DNA bases **5** and **9** (Scheme 2). The IR spectrum for compound **4** confirms the disappearance of -NH₂ peak and a carbonyl group at 1700 cm⁻¹. The ¹H-NMR spectrum shows two singlets at 1.05 ppm (s, 3H, -CH₃) and 1.07 ppm (s, 3H, -CH₃) for the new two methyl groups. The IR spectrum of compound **5** confirms the disappearance of -OH. The ¹H-NMR also confirms the disappearance of OH proton and it shows two singlets at δ ppm, 3.68 ppm (s, 3H, -OCH₃) and 3.70 ppm (s, 3H, -OCH₃) for the two methoxy groups of DMT.

6-Amino-thiouracile **10** synthesized with a known procedure [28] was allowed to react with carbon disulphide



Scheme 1



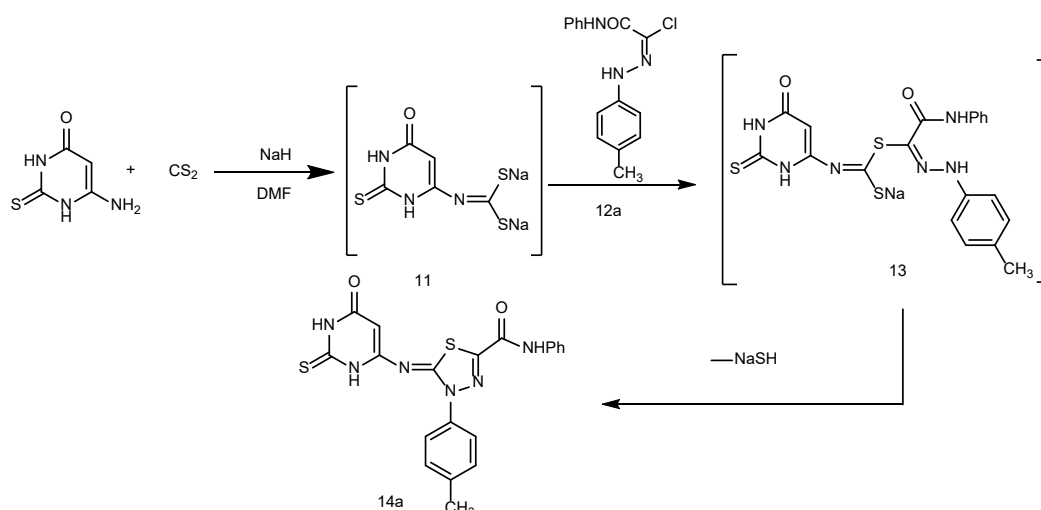
Scheme 2

in the presence of sodium hydride to yield the non-soluble disodium salt **11**. The addition of hydrazonoyl halide [29] **12a** to the formed salt **11** furnished the final isolated product **14a** (Scheme 1). The $^1\text{H-NMR}$ spectrum of **14a** revealed the presence of a singlet signal at $\delta = 5.34$ ppm corresponding to the pyrimidine hydrogen besides the characteristic signals of the aromatic protons at $\delta = 7.15$ – 7.62 , 7.82 , 7.96 ppm and three signals attributed to the $-\text{NH}$ protons at $\delta = 11.74$, 12.08 and 14.02 ppm (c.f. exp. Section). All the other spectroscopic and analytical data were in

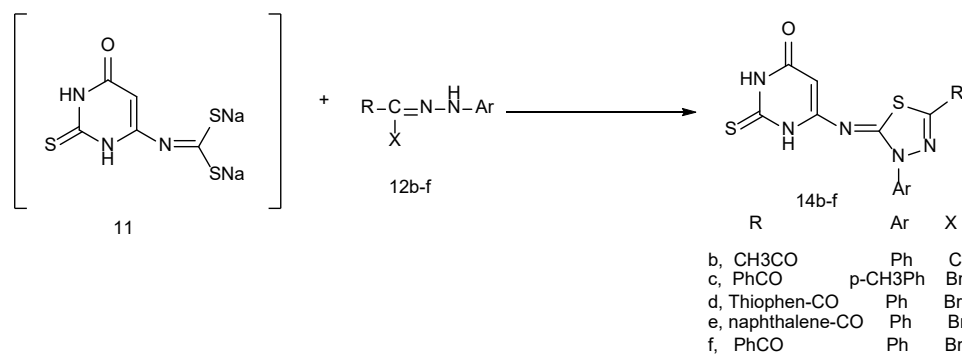
accordance with the suggested structure **14a** (Scheme 3).

It is believed that the addition of hydrazonoyl halide **12a** to the dithioimidacarbonate salt **11** led to the intermediate adduct **13**. The latter intermediate was cyclized *via* loss of NaSH to form the final cyclized product **14a**.

To generalize such methodology, the previous reaction was carried out by the use of different hydrazonoyl halide derivatives **12b-f** to yield the corresponding isolated products **14b-f** (Scheme 4). The



Scheme 3



Scheme 4

structures of all products were confirmed by spectroscopic and analytical data (c.f. experimental section).

Treatment of 6-amino-2-thiouracil with phenyl isothiocyanate in DMF containing KOH with stirring afforded the non-isolated potassium salt **16**. Interaction of **16** with different halogenated reagents did not produce the expected thiazole derivatives. The reaction yielded the products **18** upon using CH₃COCl or chloroacetonitrile that revealed the fast hydrolysis of the salt before addition. Use of benzoylchloride produced the open addition product **19** (Scheme 5).

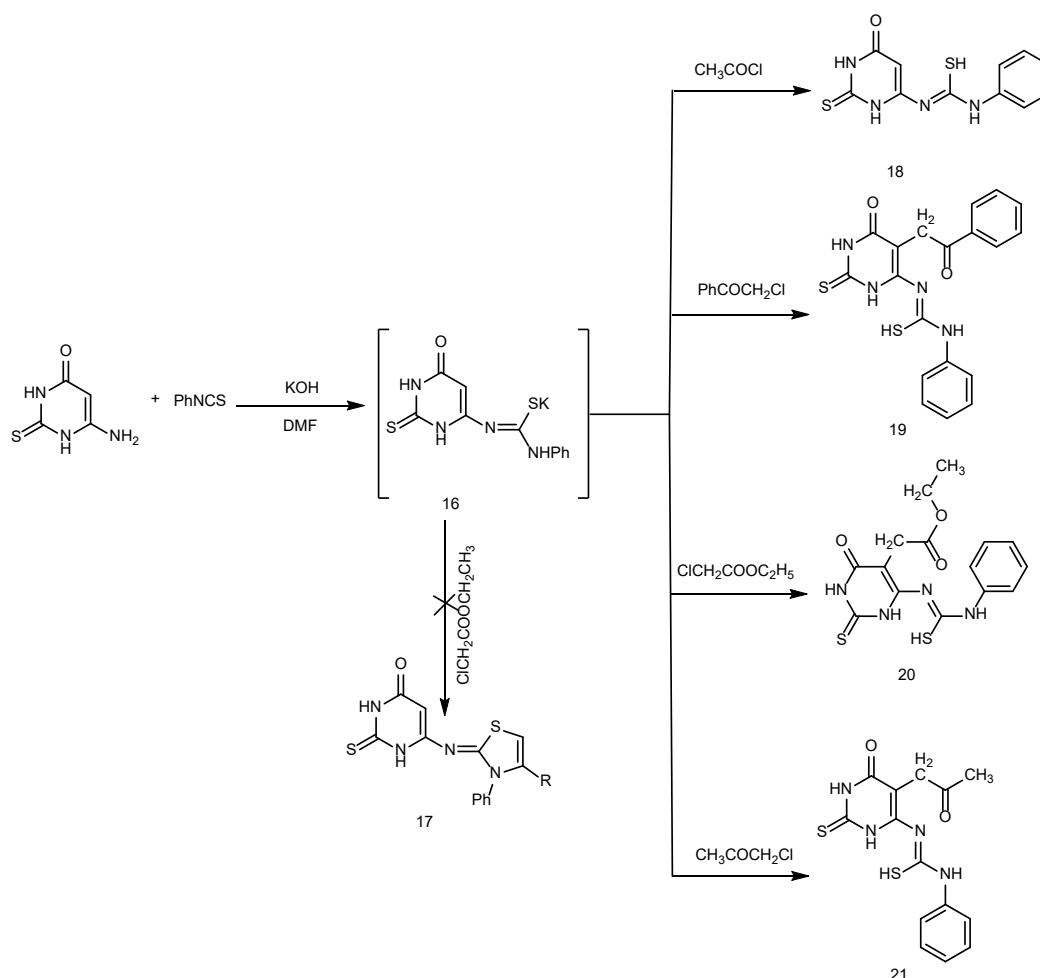
All the spectroscopic data confirmed the suggested structure (c.f. experimental section).

Molecular Docking Results

To test our docking proposal and to ensure that the binding poses of the docked ligands represented favorable and valid potential binding modes, the docking parameters

and methods were validated by redocking the cocrystal ligand in order to determine the ability of Auto Dock vina to reproduce the orientation and position of the ligand observed in the crystal structure. The redocking of cocrystal ligands to their respective molecular targets exhibited an RMSD value of < 2 Å between the original cocrystal ligand position and the docked poses, as the RMSD were 1.047 Å for 1DI8 receptor and 1.343 Å for 2O2F receptor (Fig. 1). This confirmed that the ligands were closely bound to the true conformation of their targets indicating the reliability of the docking protocols and parameters [42].

The molecular docking studies revealed that the compounds **14e**, **14f**, **14c**, **14a**, **19**, and **14d** were the most promising compounds, which is explained by their low binding energies (-9.6, -9.5, -9.0, -8.9, -8.8, and -8.6 kcal/mol, respectively), hydrogen bonding and hydrophobic interactions with the active site residues of



Scheme 5

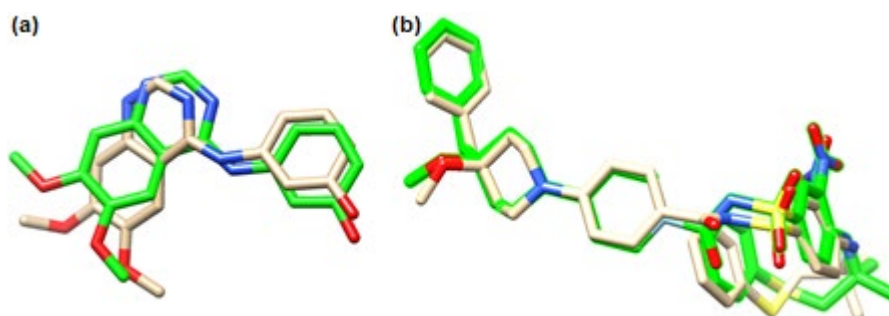


Fig 1. Docking was validated by redocking the cocrystal ligands to their corresponding receptors. The original conformation of each cocrystal ligands is displayed in a green stick, while docked poses are represented in a grey stick. The root means square deviation (RMSD) was calculated between the original and docked poses of the cocrystal ligands. (a) RMSD: 1.047Å (PDB ID: 1DI8); (b) RMSD: 1.343Å (PDB ID: 2O2F) using Chimera software

CDK-2 shown in Table 1 and 2, and Fig. 2. While compounds **14e**, **14c**, **19**, and **14a** were the most active compounds against BCL-2, which is depicted by the low binding energies (-8.2, -8.1, -8.1, and -8.1 kcal/mol,

respectively) shown in Table 1 and 3, and Fig. 3. Our molecular analysis revealed that compound **14e** was the most active compound against both proteins and that might be due to the incorporation of the free sulphur

atom (C=S) and the two nitrogens (2NH) in the pyrimidine ring. This lead to better binding of compound **14e** with the pocket of CDK-2, as depicted by 7 hydrogen bonds formation with the amino acids residues in the pocket GLN131.A (bond length 3.909 Å), ASN132.A (bond length 3.452 Å), ASN131.A (bond length 3.226 Å), GLN131.A (bond length 3.516 Å), THR14.A (bond length 2.922 Å), ASP145.A (bond length 3.461 Å), and LYS33.A (bond

length 3.133 Å).

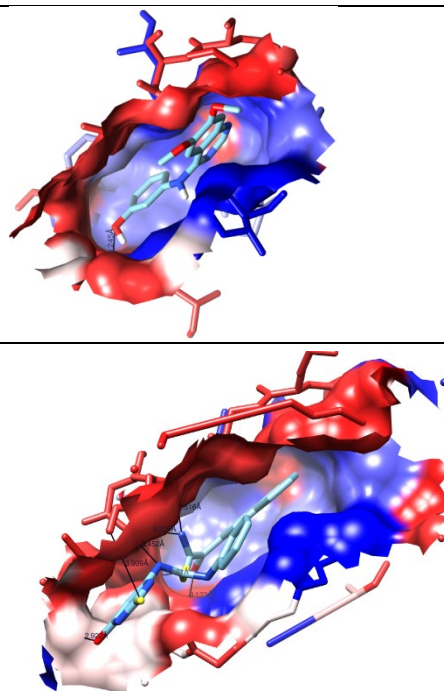
Moreover, compound **14c** was able to form 2 hydrogen bonds with the amino acids residues in the pocket of BCL-2 protein ALA97.A (bond length 3.031 Å), and TRP141.A (bond length 2.471 Å). These results shed a light on compound **14e** as a promising anticancer agent, and further wet lab experiments should be done to verify its activity.

Table 1. The results of molecular docking of best conformer with CDK-2 (1di8) receptor

Drugs	Free energy of binding (Kcal/mol)	
	CDK2	BCL2
Reference ligand	-8.3	-10.6
14a	-8.9	-8.1
14b	-8.1	-6.7
14c	-9.0	-8.1
14d	-8.6	-7.3
14e	-9.6	-8.2
14f	-9.5	-7.7
18	-7.5	-6.4
19	-8.8	-8.1
20	-7.5	-6.3
21	-8.0	-6.8

Table 2. The Hydrophobic interactions of best conformer with CDK-2 (1di8) receptor

Compounds	Hydrophobic interactions
Reference ligand	ILE10, VAL18, LEU148, VAL64, LEU134, LEU83
14e	ILE10, VAL18, LEU148, VAL64, LEU134, LEU83, PHE82, LEU298



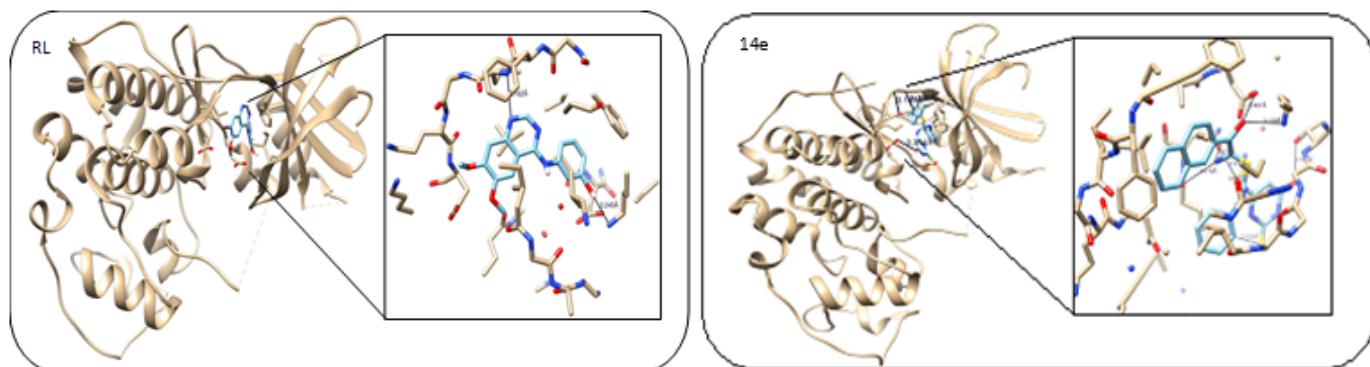


Fig 2. 3D of hydrogen bond interaction between reference ligand (RL), and the most promising compound (**14e**) with CDK-2 protein

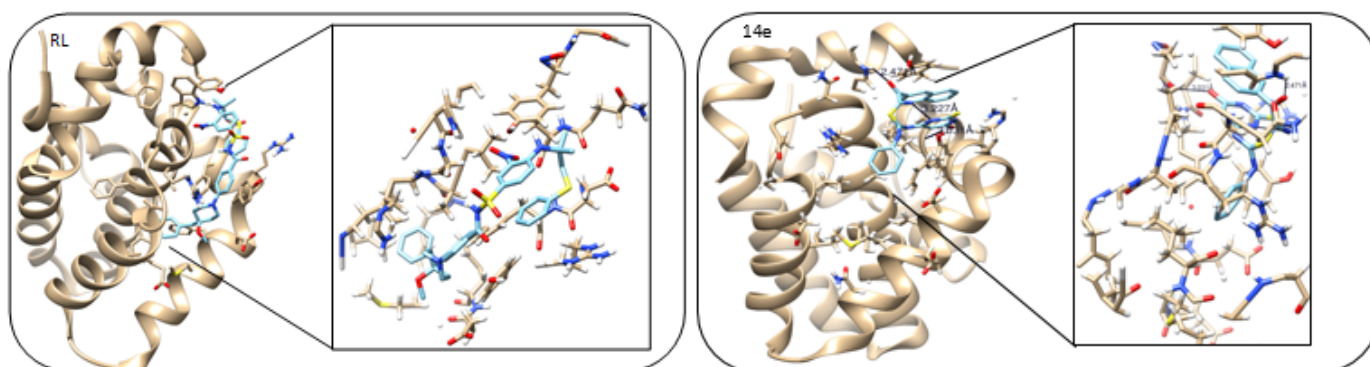
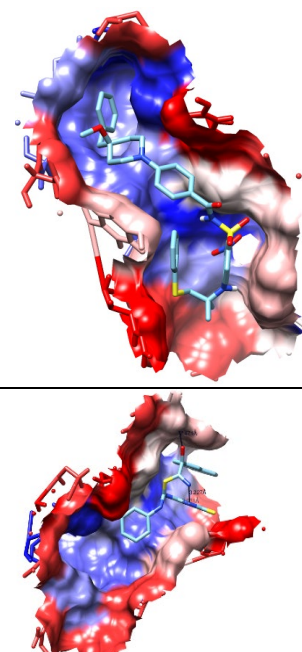


Fig 3. 3D of hydrogen bond interaction between reference ligand (RL), and the most promising compound (**14e**) with BCL-2 protein

Table 3. The Hydrophobic interactions of best conformer with BCL-2 (2O2F) receptor

Compounds	Hydrophobic interactions
Reference ligand	MET112, VAL130, VAL145, LEU134, ALA146, PHE101, PHE109, PHE150
14e	MET112, VAL130, VAL145, LEU134, PHE101, PHE109, PHE150, PHE147



■ CONCLUSION

The presented work has described the chemical modification of the pyrimidine ring base of heterocyclic biologically active compounds. Docking studies for these compounds as anticancer agents have been carried out, in order to gain insights into their binding modes against cyclin-dependent protein kinase 2 (CDK-2) that is involved in cell cycle and receptor protein B-cell lymphoma 2 (BCL-2) that is involved in cell apoptosis. These targets have been selected based on their key roles in cancer progression via the regulation of the cell cycle and DNA replication.

■ REFERENCES

- [1] Cogoi, S., Ferino, A., Miglietta, G., Pedersen, E.B., and Xodo, L.E., 2018, The regulatory G4 motif of the Kirsten ras (KRAS) gene is sensitive to guanine oxidation: Implications on transcription, *Nucleic Acids Res.*, 46 (2), 661–676.
- [2] Kosbar, T.R., Sofan, M.A., Waly, M.A., and Pedersen, E.B., 2015, Anti-parallel triplexes: Synthesis of 8-aza-7-deazaadenine nucleosides with a 3-aminopropynyl side-chain and its corresponding LNA analog, *Bioorg. Med. Chem.*, 23 (10), 2458–2469.
- [3] Müller, P., Rößler, J., Schwarz-Finsterle, J., Pedersen, E.B., Géci, I., Schmitt, E., and Hausmann, M., 2017, Corrigendum to “PNA-COMBO-FISH: From combinatorial probe design in silico to vitality compatible, specific labelling of gene targets in cell nuclei” [Exp. Cell Res., 345 (2016), 51–59], *Exp. Cell Res.*, 355 (2), 194–195.
- [4] Gouda, A.S., Amine, M.S., and Pedersen, E.B., 2017, Synthesis and molecular modeling of thermally stable DNA G-quadruplexes with anthraquinone insertions, *Eur. J. Org. Chem.*, 2017 (21), 3092–3100.
- [5] El-Sayed, A.A., Pedersen, E.B., and Khaireldin, N.Y., 2016, Thermal stability of modified i-motif oligonucleotides with naphthalimide intercalating nucleic acids, *Helv. Chim. Acta*, 99 (1), 14–19.
- [6] El-Sayed, A.A., Pedersen, E.B., and Khaireldin, N.A., 2012, Studying the influence of the pyrene intercalator TINA on the stability of DNA i-motifs, *Nucleosides Nucleotides Nucleic Acids*, 31 (12), 872–879.
- [7] Cogoi, S., Jakobsen, U., Pedersen, E.B., Vogel, S., and Xodo, L.E., 2016, Lipid-modified G4-decoy oligonucleotide anchored to nanoparticles: Delivery and bioactivity in pancreatic cancer cells, *Sci. Rep.*, 6, 38468.
- [8] Pabon-Martinez, Y.V., Xu, Y., Villa, A., Lundin, K.E., Geny, S., Nguyen, C.H., Pedersen, E.B., Jørgensen, P.T., Wengel, J., Nilsson, L., Smith, C.I.E., and Zain, R., 2017, LNA effects on DNA binding and conformation: From single strand to duplex and triplex structures, *Sci. Rep.*, 7 (1), 11043.
- [9] Bredy, T.W., 2017, *DNA Modifications in the Brain*, Academic Press, USA.
- [10] Khan, Z.U., and Muly, E.C., 2014, *Molecular Basis of Memory*, Progress in Molecular Biology and Translational Science Series, Vol. 122, Academic Press, USA.
- [11] Mohamed, N.R., Khaireldin, N.Y., Fahmy, A.F., and El-Sayed, A.A., 2010, Facile synthesis of fused nitrogen containing heterocycles as anticancer agents, *Der Pharma Chem.*, 2 (1), 400–417.
- [12] Hu, C., Chen, X., Zhao, W., Chen, Y., and Huang, Y., 2016, Design and modification of anticancer peptides, *Drug Des.*, 5 (3), 1000138.
- [13] Fan, J., Wang, S., Sun, W., Guo, S., Kang, Y., Du, J., and Peng, X., 2018, Anticancer drug delivery systems based on inorganic nanocarriers with fluorescent tracers, *AIChE J.*, 64 (3), 835–859.
- [14] Qian, Y., Bi, L., Yang, Y., and Wang, D., 2018, Effect of pyruvate kinase M2-regulating aerobic glycolysis on chemotherapy resistance of estrogen receptor-positive breast cancer, *Anticancer Drugs*, 29 (7), 616–627.
- [15] Caton-Williams, J., Lin, L., Smith, M., and Huang, Z., 2011, Convenient synthesis of nucleoside 5'-triphosphates for RNA transcription, *Chem. Commun.*, 47 (28), 8142–8144.
- [16] Lin, C.X., Fu, H., Tu, G.Z., and Zhao, Y.F., 2004, Synthesis of AZT/d4T boranophosphates as anti-HIV prodrug candidates, *Synthesis*, 2004 (4), 509–516.
- [17] Lin, C.X., Fu, H., Tu, G.Z., and Zhao, Y.F., 2010, Novel and convenient approach to synthesis of

- AZT/d4T H-phosphonates, *Chin. J. Chem.*, 22 (3), 225–227.
- [18] Gadhula, S., Chu, C.K., and Schinazi, R.F., 2005, Synthesis and anti-HIV activity of β -D-3'-azido-2',3'-unsaturated nucleosides and β -D-3'-azido-3'-deoxyribofuranosylnucleosides, *Nucleosides Nucleotides Nucleic Acids*, 24 (10-12), 1707–1727.
- [19] Sun, X.B., Kang, J.X., and Zhao, Y.F., 2002, One-pot synthesis of hydrogen phosphonate derivatives of d4T and AZT, *Chem. Commun.*, 20, 2414–2415.
- [20] Loksha, Y.M., Pedersen, E.B., Loddo, R., and La Colla, P., 2016, Synthesis and anti-HIV-1 evaluation of some novel MC-1220 analogs as non-nucleoside reverse transcriptase inhibitors, *Arch. Pharm.*, 349 (5), 363–372.
- [21] Flefel, E.M., Tantawy, W.A., El-Sofany, W.I., El-Shahat, M., El-Sayed, A.A., and Abd-Elshafy, D.N., 2017, Synthesis of some new pyridazine derivatives for anti-HAV evaluation, *Molecules*, 22 (1), E148.
- [22] El-Sayed, A.A., Tamara Molina, A., Álvarez-Ros, M.C., and Alcolea Palafox, M., 2015, Conformational analysis of the anti-HIV Nikavir prodrug: Comparisons with AZT and Thymidine, and establishment of structure-activity relationships/tendencies in other 6'-derivatives, *J. Biomol. Struct. Dyn.*, 33 (4), 723–748.
- [23] Yaqub, G., Hussain, E.A., and Mateen, B., 2010, Synthetic approaches to lamivudine: An anti-HIV AIDs and anti-hepatitis B drug, *Asian J. Chem.*, 22, 4962–4968.
- [24] Caso, M.F., D'Alonzo, D., D'Errico, S., Palumbo, G., and Guaragna, A., 2015, Highly stereoselective synthesis of lamivudine (3TC) and emtricitabine (FTC) by a novel N-glycosidation procedure, *Org. Lett.*, 17 (11), 2626–2629.
- [25] Hu, Y.Q., Zhang, S., Xu, Z., Lv, Z.S., Liu, M.L., and Feng, L.S., 2017, 4-Quinolone hybrids and their antibacterial activities, *Eur. J. Med. Chem.*, 141, 335–345.
- [26] Rizk, S.A., El-Naggar, A.M., and El-Badawy, A.A., 2018, Synthesis, spectroscopic characterization and computational chemical study of 5-cyano-2-thiouracil derivatives as potential antimicrobial agents, *J. Mol. Struct.*, 1155, 720–733.
- [27] Sahu, M., Siddiqui, N., Iqbal, R., Sharma, V., and Wakode, S., 2017, Design, synthesis, and evaluation of newer 5,6-dihydropyrimidine-2(1H)-thiones as GABA-AT inhibitors for anticonvulsant potential, *Bioorg. Chem.*, 74, 166–178.
- [28] Bhalgat, C.M., Ali, M.I., Ramesh, B., and Ramu, G., 2014, Novel pyrimidine and its triazole fused derivatives: Synthesis and investigation of antioxidant and anti-inflammatory activity, *Arabian J. Chem.*, 7 (6), 986–993.
- [29] Zhang, Q., Luo, J., Ye, L., Wang, H., Huang, B., Zhang, J., Wu, J., Zhang, S., and Tian, Y., 2014, Design, synthesis, linear and nonlinear photophysical properties and biological imaging application of a novel Λ -type pyrimidine-based thiophene derivative, *J. Mol. Struct.*, 1074, 33–42.
- [30] Sukach, V.A., Tkachuk, V.M., Rusanov, E.B., Rösenthaler, G.V., and Vovk, M.V., 2012, Heterocyclization of N-(1-chloro-2,2,2-trifluoroethylidene)carbamates with β -enaminoesters—a novel synthetic strategy to functionalized trifluoromethylated pyrimidines, *Tetrahedron*, 68 (40), 8408–8415.
- [31] Mohamed, M.F., Hassaneen, H.M., and Abdelhamid, I.A., 2018, Cytotoxicity, molecular modeling, cell cycle arrest, and apoptotic induction induced by novel tetrahydro-[1,2,4]triazolo[3,4-a]isoquinoline chalcones, *Eur. J. Med. Chem.*, 143, 532–541.
- [32] Yahya, S.M.M., Abdelhamid, A.O., Abd-Elhalim, M.M., Elsayed, G.H., and Eskander, E.F., 2017, The effect of newly synthesized progesterone derivatives on apoptotic and angiogenic pathway in MCF-7 breast cancer cells, *Steroids*, 126, 15–23.
- [33] Brahmachari, G., 2015, *Green Synthetic Approaches for Biologically Relevant Heterocycles*, Elsevier, Boston, USA.
- [34] Mohamed, N.R., El-Saidi, M.M.T., Ali, Y.M., and Elnagdi, M.H., 2007, Utility of 6-amino-2-thiouracil as a precursor for the synthesis of

- bioactive pyrimidine derivatives, *Bioorg. Med. Chem.*, 15 (18), 6227–6235.
- [35] El-Sayed, A.A., Khaireldin, N.Y., El-Shahat, M., Elhefny, E.A., El-Saidi, M.M.T., Ali, M.M., and Mahmoud, A.E., 2016, Anti proliferative activity for newly heterofunctionalized pyridine analogues, *Ponte*, 72 (7), 106–18.
- [36] Patel, H.V., Vyas, K.A., Pandey, S.P., and Fernandes, P.S., 1996, Facile synthesis of hydrazonyl halides by reaction of hydrazones with *N*-halosuccinimide-dimethyl sulfide complex, *Tetrahedron*, 52 (2), 661–668.
- [37] Shawali, A.S., Farag, A.M., Albar, H.A., and Dawood, K.M., 1993, Facile syntheses of bi-1,2,4-triazoles via hydrazonyl halides, *Tetrahedron*, 49 (13), 2761–2766.
- [38] El-Gohary, N.S., and Shaaban, M.I., 2018, Design, synthesis, antimicrobial, antiquorum-sensing and antitumor evaluation of new series of pyrazolopyridine derivatives, *Eur. J. Med. Chem.*, 157, 729–742.
- [39] Sebeka, A.A.H., Osman, A.M.A., El Sayed, I.E.T., El Bahanasawy, M., and Tantawy, M.A., 2017, Synthesis and antiproliferative activity of novel neocryptolepine-hydrazides, *J. Appl. Pharm. Sci.*, 7 (10), 9–15.
- [40] Nasab, M.J., Kiasat, A.R., and Zarasvandi, R., 2018, β -Cyclodextrin nanosponge polymer: A basic and eco-friendly heterogeneous catalyst for the one-pot four-component synthesis of pyranopyrazole derivatives under solvent-free conditions, *React. Kinet. Mech. Catal.*, 124 (2), 767–778.
- [41] Saeidi, Z., and Vatandoost, H., 2018, Aquatic insect from Iran for possible use of biological control of main vector-borne disease of malaria and water indicator of contamination, *J. Arthropod Borne Dis.*, 12 (1), 1–15.
- [42] Bursulaya, B.D., Totrov, M., Abagyan, R., and Brooks, C.L., 2003, Comparative study of several algorithms for flexible ligand docking, *J. Comput. Aided Mol. Des.*, 17 (11), 755–763.